超声多模态检查可提高对乳腺非肿块型病变的诊断效能[*]

王慧妍， 陆龙颖， 张和庆， 万　雪， 何玉霜， 骆洪浩， 彭玉兰， 马　琳， 赵海娜[△]

四川大学华西医院 超声医学科（成都 610041）

【摘要】 目的　本研究的超声多模态检查是指高频超声（ultrasound, US）、声辐射力脉冲成像（acoustic radiation force impulse, ARFI）、超声造影（contrast-enhanced ultrasound, CEUS）这三种超声检查方式联合使用。本研究拟分析超声多模态检查对乳腺非肿块型病变（non-mass-like lesions, NMLs）良恶性的鉴别诊断价值。方法　回顾性分析乳腺非肿块型的病例，病灶性质均经病理检查证实。依据灰阶超声图像特征，将病例分为Ⅰ～Ⅴ类型，并根据是否伴有钙化，将其中Ⅰ型及Ⅱ型又分为Ⅰa型、Ⅰb型和Ⅱa型、Ⅱb型，统计分析各分型恶性比例。建立US、US+ARFI、US+CEUS、US+ARFI+CEUS的logistic诊断恶性病例的回归模型，绘制受试者工作特征（ROC）曲线，计算曲线下面积（area under the curve, AUC），并进行比较。分析US、ARFI与CEUS串联实验对不伴钙化的恶性NMLs（不典型恶性NMLs）的检出率。结果　最终纳入研究病例407例，均为女性，年龄22～81岁，平均年龄（47.0±11.0）岁。其中良性病例220例，恶性病例187例。恶性占比从高到低分别为Ⅰb型>Ⅱb型>Ⅲ型>Ⅴ型>Ⅰa型>Ⅱa型>Ⅳ型，伴有钙化的低回声区恶性比例明显高于不伴钙化的病灶。US、US+ARFI、US+CEUS、US+ARFI+CEUS的logistic回归模型诊断恶性病例的AUC及95%置信区间（CI）分别为0.895（0.862～0.927）、0.908（0.878～0.937）、0.921（0.893～0.948）、0.927（0.902～0.952）。4个回归模型的AUC相比，差异有统计学意义（P<0.001）。US对不伴钙化的NMLs的检出率为80.7%，若US与CEUS、ARFI联合，当病灶CEUS评分为4分或5分或ARFI中的剪切波速度（shear-wave velocity, SWV）≥4.28 m/s时判断为恶性，此时可以检出86.4%的不伴钙化的恶性NMLs病灶。结论　伴有钙化的乳腺NMLs恶性风险高，均建议行病理学检查明确诊断；不伴钙化的乳腺NMLs可以联合多模态超声检查，有助于提高诊断效能。

【关键词】　声辐射力脉冲成像　　超声造影　　高频超声　　乳腺病变　　非肿块型

Ultrasound Multimodality Examination Improves the Diagnostic Efficiency of Non-Mass-Like Breast Lesions

WANG Huiyan, LU Longying, ZHANG Heqing, WAN Xue, HE Yushuang, LUO Honghao, PENG Yulan, MA Lin, ZHAO Haina[△]. Department of Ultrasound, West China Hospital, Sichuan University, Chengdu 610041, China

△ Corresponding author, E-mail: 2320844137@qq.com

【**Abstract**】　**Objective**　This study is focused on ultrasound multimodality examination, which refers to the combined use of three ultrasound examination modalities, ultrasound (US), acoustic radiation force impulse (ARFI) imaging, and contrast-enhanced ultrasound (CEUS). The purpose of this study is to analyze the value of applying ultrasound multimodality examination in the differential diagnosis of benign and malignant breast non-mass-like lesions (NMLs). **Methods**　Cases of breast NMLs were analyzed retrospectively, and the nature of all the lesions was verified by pathological examination. Based on the gray-scale ultrasound image characteristics, the cases were classified into types Ⅰ to Ⅴ, and type Ⅰ and type Ⅱ were further classified into 4 subtypes, Ⅰa, Ⅰb, Ⅱa, and Ⅱb, according to whether there was also calcification, and the proportion of malignant cases in each subtype was statistically analyzed. Logistic regression models of US, US+ARFI, US+CEUS, and US+ARFI+CEUS for the diagnosis of malignant cases were established, ROC curves were drawn, the area under the curve (AUC) was calculated, and comparisons were made accordingly. The detection rate of malignant NMLs without calcification (atypical malignant NMLs) by the combination examination of US, ARFI, and CEUS was analyzed. **Results**　A total of 407 cases were included in the study. All subjects were female, aged 22 to 81 years, with the average age being (47.0±11.0) years. There were 220 benign cases and 187 malignant cases. Ranked from the highest to the lowest, the malignancy proportion of the different types was Ⅰb>Ⅱb>Ⅲ>Ⅴ>Ⅰa>Ⅱa>Ⅳ. The malignant proportion of the low echo area with calcification was significantly higher than that of the lesions without calcification. The AUC (95% confidence interval [CI]) for diagnosing malignant cases with the logistic regression models of US, US+ARFI, US+CEUS, and US+ARFI+CEUS were 0.895 (0.862-0.927), 0.908 (0.878-0.937), 0.921 (0.893-0.948), and 0.927 (0.902-0.952), respectively. Comparison of the AUC of the 4 regression models showed significant differences (P<0.001). The detection rate of US for NMLs without calcification was 80.7%.

When US was used in combination with ARFI and CEUS, 86.4% of the malignant NMLs lesions without calcification could be detected if the lesion CEUS score was 4 or 5 points or if shear-wave velocity (SWV)≥4.28 m/s. **Conclusion** Breast NMLs with calcification show high risks of malignancy, and a pathological examination is always recommended for a conclusive diagnosis. Ultrasound multimodality examination can improve the diagnostic accuracy of breast NML without calcification.

【Key words】　　Acoustic radiation force impulse　　Contrast-enhanced ultrasound　　Ultrasound　　Breast lesions　　Non-mass-like

超声检查是乳腺病变最重要的影像学方法之一。根据超声图像的特征,乳腺病灶可以分为肿块型和非肿块型病变两种。乳腺非肿块型病变(non-mass-like lesions, NMLs)是指病变在超声图像上未呈现明确的边界,而且在两个不同的扫查方向上不具备空间占位效应[1-2]。由于BI-RADS评估分类中未纳入乳腺NMLs,且此类病灶没有占位效应,导致NMLs的检出和良恶性鉴别诊断成为临床工作的难点。超声多模态检查通过联合高频超声、弹性超声和超声造影等技术,多方位评估病灶,可能有助于NMLs性质的判断。目前临床上用的弹性超声主要有3种,声辐射力脉冲成像(acoustic radiation force impulse, ARFI)是其中的一种。ARFI的工作原理是通过声辐射力施予组织一定压力,终止后记录组织形变,再转换成为黑白弹性图的一种模式,包括声触诊组织成像(virtual touch tissue imaging, VTI)和声触诊组织定量(virtual touch tissuequantification, VTQ)。VTIQ(virtual touch tissue imaging quantification)是VTQ和VTI的联合使用。本研究拟通过回顾性分析乳腺NMLs的高频超声(ultrasound, US)、ARFI和超声造影(contrast-enhanced ultrasound, CEUS)的图像特征,评估超声多模态检查评估乳腺NMLs性质的应用价值。

1　资料与方法

1.1　研究对象

回顾性分析2019年3月–2022年8月于四川大学华西医院行乳腺超声多模态检查的病例。纳入标准: ①超声图像均采用西门子ACUSONO xanal彩色超声诊断仪采集; ②均进行了US、VTIQ和CEUS检查; ③病灶区不符合BI-RADS标准中的 "肿块" 的定义, 为超声NMLs的表现; ④病灶性质均经病理检查证实。排除标准: ①超声多模态检查资料不完整者; ②病灶病理结果不明确者。本研究获四川大学华西医院生物医学伦理审查委员会批准, 批准号2021年审(1965)号。

1.2　仪器与方法

1.2.1　常规US检查

使用德国西门子ACUSONO xanal彩色多普勒超声诊仪,乳腺病灶US图像使用L18-5线阵探头采集,记录病灶的大小、钙化、内部及后方回声,腋窝淋巴结结构是否异常。当腋窝淋巴结皮质厚度>2 mm、淋巴门消失、伴有液化或钙化时,判定为淋巴结结构异常[3-4]。采集彩色多普勒图像及频谱多普勒图像,记录病灶内动脉收缩期峰值流速(PSV)、阻力指数(RI)。

1.2.2　CEUS检查

采用L9-4线阵探头进行CEUS检查。造影剂为意大利Bracco公司生产的SonoVue冻干粉。首先用5 mL生理盐水溶解并震荡摇匀,经肘正中静脉团注SonoVue混悬液4.8 mL,随后快速推注5 mL生理盐水冲管,同时启动计时及造影视频录制,实时观察病灶内造影剂分布情况,分析病灶造影增强模式。

CEUS评分参考罗葆明团队的研究[5]。病灶无增强评为1分,与周围腺体组织相比,病灶峰值强度与周围组织相近、无明显边界时评为2分,病灶呈均匀或不均匀高增强、增强后形状大小与灰阶超声无变化评分3分,病灶增强后范围较灰阶超声扩大评为4分,病灶增强后呈蟹足状或有坏死区评为5分。

1.2.3　VTIQ

采用L9-4线阵探头进行ARFI检查。选择垂直导管方向的断面,嘱患者屏气,采集速度模式和质控模式图像,将速度模式图像量程调节为10 m/s,测量病灶质硬区剪切波速度(shear-wave velocity, SWV)5次,计算5次测量的平均值。测量病灶同深度区正常腺体内SWV 1次。

1.2.4　NMLs超声图像再次读图

目前尚无明确的指南或专家共识提出乳腺NMLs的超声分类标准。HSU等[6]的研究在超声专业内讨论乳腺NMLs时引用者较多,所以本研究参考这篇文献,依据超声图像表现,将乳腺NMLs的超声图像特征分为4种类型。Ⅰ型为导管样低回声区,其中Ⅰa型不伴微钙化,Ⅰb型伴有微钙化; Ⅱ型为非导管样片状低回声区,其中Ⅱa型不伴微钙化,Ⅱb型伴有微钙化; Ⅲ型表现为结构扭曲,Ⅳ型表现为声影,但无明显肿块回声。另外,本研究将病灶区回声与周围乳腺组织无异、但可见少许点状强回声者归为Ⅴ类。

1.2.5　纳入分析的超声征象

　　纳入分析的US的图像征象包括超声分型、钙化、周围组织改变、后方回声、病灶血流分级、血流频谱及腋窝淋巴结结构是否异常7个征象;ARFI包括病灶区弹性测值和病灶区与周围组织弹性比值2个征象;CEUS包括造影评分1个征象。

1.3　统计学方法

　　采用SPSS27.0统计软件进行数据分析。符合正态分布的计量资料采用t检验,不符合正态分布的计量资料采用秩和检验;计数资料采用行×列表的卡方检验,以病理检查为金标准,分析US、ARFI及CEUS多种模态的不同超声征象在乳腺良、恶性病变中的比例差异,当$P<0.05$时,差异有统计学意义,计算各个征象的比值比(OR)值。最后将差异有统计学意义的征象纳入多因素logistic回归分析,设置α和β值分别为0.05和0.1,通过逐步前进法查找预测病灶良恶性的独立影响因素,并构建多因素分析预测模型。建立US、US+ARFI、US+CEUS及US+ARFI+CEUS的logistic回归模型,绘制受试者工作特征(ROC)曲线,计算曲线下面积(area under the curve, AUC),评估模型的诊断价值。

2　结果

2.1　NMLs分型分布及恶性占比

　　共565例NMLs病例,其中107例无病理结果或病理结果不明,36例无弹性定量分析,弹性测量未采用VTIQ的15例,予以删除,最终纳入研究病例407例,均为女性,年龄22～81岁,平均年龄(47.0±11.0)岁。见表1。其中良性病例220例,恶性病例187例。恶性病例占比从高到低分别为Ⅰb型>Ⅱb型>Ⅲ型>Ⅴ型>Ⅰa型>Ⅱa型>Ⅳ型。

表1　NMLs病例超声分型及恶性占比
Table 1　The ultrasonic classification and malignancy proportion of the NMLs cases

Type	Total (n=407)	Malignance (n=187)	Benignity (n=220)	Malignancy proportion
Ⅰa	99	25	74	25.3%
Ⅰb	96	79	17	82.3%
Ⅱa	107	24	83	22.4%
Ⅱb	54	42	12	77.8%
Ⅲ	18	8	10	44.4%
Ⅳ	17	2	15	11.8%
Ⅴ	16	7	9	43.8%

2.2　NMLs超声图像特征恶性风险

　　本研究结果显示不同超声图像特征恶性风险比较见

表2,其中伴有结构扭曲、后方回声衰减、腋窝淋巴结异常、高增强、钙化、造影评分为4分或5分、弹性测值≥4.28 m/s的病例恶性风险更高。各个征象OR值由高到低排序为高增强>微钙化>弹性测值>腋窝淋巴结异常>结构扭曲>后方回声衰减,说明表现为高增强的病灶恶性风险最高。典型恶性NML图片见图1。

2.3　多模态logistic回归分析模型在NMLs中诊断恶性病例的ROC曲线

　　将单因素分析差异有统计学意义的征象纳入logistic回归分析,设Y为病理确诊的NMLs恶性例数(1=恶性例

表2　非肿块型病变超声征象
Table 2　Ultrasonic signs of non-mass-like lesions

Ultrasonic image feature	n	Malignancy	Benignity	Odds ratio	P
Average age/yr.		49.3	45.2		<0.001
Distorted structure/case					<0.001
Yes	160	115	45	6.21	
None	247	72	175		
Posterior echo/case					0.128
Attenuation	184	114	70	3.35	
No attenuation	223	73	150		
CEUS/case					<0.001
High enhancement	254	173	81	21.21	
Other enhancement	153	14	139		
Contrast score/case					<0.001
5 points	88	71 (80.7%)[*]	17		
4 points	97	76 (79.2%)[*]	21		
3 points	69	26 (37.7%)[*]	43		
2 points	136	13 (9.6%)[*]	123		
1 poins	17	1 (5.9%)[*]	16		
Axillary lymph nodes/case				6.22	0.021
Abnormal	114	87	27		
Normal	293	100	193		
Elastic score/case					<0.001
≥4.28 m/s	178	129	50	7.56	
<4.28 m/s	229	58	170		
Calcification/case					<0.001
Micro-calcification	166	129	38	10.65	
None	241	58	182		
Peak systolic velocity/case				9.89	<0.001
≥15.9 cm/s	75	64	11		
<15.9 cm/s	332	123	209		

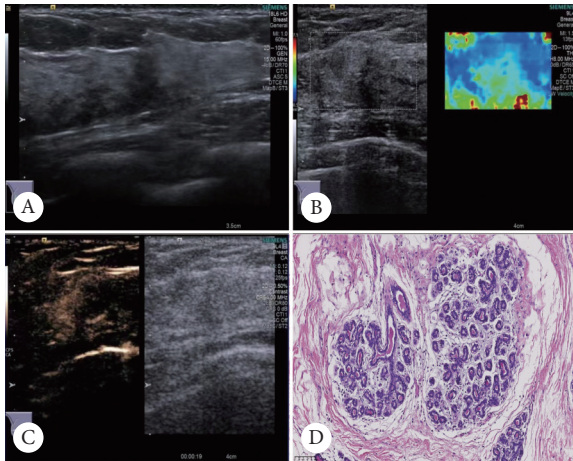[*] Malignancy proportion in brackets.

图 1　同一患者的恶性 NML在不同检查方法中的表现

Fig 1　Manifestations of malignant NML in the same patient by different examination methods

　　A, US image, type Ⅳ lesions of invasive breast cancer; B, ARFI image, SWV=3.08 m/s; C, CEUS image, with the CEUS score being 4 points; D, pathological image of HE staining (original magnification ×20).

数增加; 0= 恶性例数减少), 分别建立US+ARFI、US+CEUS、US+ARFI+CEUS多模态超声的logistic回归模型, 纳入的X见表3。US的logistic回归模型分析纳入的X为: 结构扭曲(X_1, 0= 无结构扭曲, 1= 结构扭曲)、年龄(X_2,

0= 49岁以下, 1= 49岁以上)、分型(X_3, 0= Ⅰa、Ⅱa、Ⅲ、Ⅳ、Ⅴ型, 1= Ⅰb、Ⅱb)、衰减(X_5, 0= 无改变和增强, 1= 衰减和混合改)、腋窝淋巴结(X_6, 0= 结构正常, 1= 结构异常)、血流分级(X_7, 0= 无、内部, 1= 周边、混合)、频谱(收缩期峰值流速)(X_8, 0= < 15.9 cm/s, 1= ≥ 15.9 cm/s)、RI(X_9, 0= < 0.7, 1= ≥0.7)。与US模型相比, US+ARFI的logistic回归模型纳入的X增加了弹性(X_{10}, 0= < 4.28 m/s, 1= ≥4.28 m/s); US+CEUS的logistic回归模型纳入的X增加了造影评分(X_4, 0= < 4分, 1= ≥4分); US+ARFI+CEUS的logistic回归模型纳入的X增加了弹性X_{10}和造影评分X_4。各logistic回归分析模型在NMLs中诊断恶性病例的ROC曲线见图2。单用US的logistic回归分析的诊断恶性病例的AUC为0.895, 95%置信区间(CI)为0.862 ~ 0.927; US+ARFI的logistic回归分析的诊断恶性病例的AUC为0.908, 95%CI为0.878 ~ 0.937; US+CEUS的logistic回归分析的诊断恶性病例的AUC为0.921, 95%CI为0.893 ~ 0.948; US+ARFI+CEUS的logistic回归分析的诊断恶性病例的AUC为0.927, 95%CI为0.902 ~ 0.952。US、US+ARFI、US+CEUS、US+ARFI+CEUS的logistic回归分析模型的AUC两两相比, 差异均有统计学意义($P< 0.001$), US联合ARFI及CEUS诊断效果最佳。

表 3　NMLs多模态超声logistic回归分析结果

Table 3　Results of the multimodal ultrasonic logistic regression analysis of NMLs

Variable	β	SE	Wald	df	P	OR	95% CI
Distorted structure (X_1)	0.684	0.350	3.818	1	0.051	1.982	0.998-3.935
Age (X_2)	1.042	0.318	10.738	1	0.001	2.836	1.520-5.290
Classification (X_3)	2.117	0.334	40.197	1	<0.000 1	8.309	4.318-15.989
Contrast score (X_4)	1.905	0.348	30.040	1	<0.000 1	6.718	3.400-13.277
Attenuation (X_5)	0.032	0.341	0.009	1	0.925	0.969	0.496-1.890
Axillary lymph nodes (X_6)	0.633	0.371	2.907	1	0.088	1.884	0.910-3.900
Blood flow classification (X_7)	0.607	0.448	1.833	1	0.176	1.884	0.762-4.420
Frequency spectrum (X_8)	0.035	0.482	0.005	1	0.943	1.035	0.402-2.664
RI (X_9)	1.095	0.455	5.781	1	0.016	2.989	1.224-7.299
AFRI imaging (X_{10})	0.866	0.345	6.315	1	0.012	2.378	1.210-4.672
Constant	3.482	0.369	88.796	1	<0.000 1	0.031	

　　β: partial regression coefficient; SE: standard error; OR: odds ratio; CI: confidence interval.

2.4　多模态检查提高对不伴钙化的恶性NMLs（不典型恶性NMLs）的检出率

　　通过上述单因素分析可知, Ⅰb和Ⅱb型病变均伴钙化, 恶性比例较高, 分别为82.3%、77.8%。不伴钙化的病例恶性比例为11.8% ~ 44.4%。US对不典型恶性病变的

检出率为80.7%, 部分不典型病例US显示不清。所以, 本研究通过联合CEUS和ARFI, 当病变CEUS评分为4分或5分或ARFI中SWV≥4.28 m/s时判断为恶性, 统计分析联合ARFI和CEUS对不伴钙化病变的恶性病变的检出率, 结果见表4。通过联合ARFI和CEUS可以检出86.4%的不典
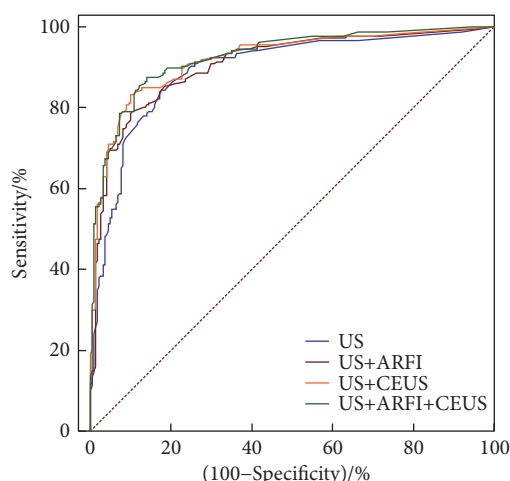
图 2　US、US+ARFI、US+CEUS、US+ARFI+CEUS的logistic回归分析的ROC曲线

Fig 2　ROC curves of US, US+ARFI, US+CEUS, and US+ARFI+CEUS

Logistic regression analysis showed statistically significant differences in the AUC of each ROC curve (*P*<0.001), with US+ARFI+CEUS showing the best diagnostic effect.

型恶性病变。

3　讨论

　　以往研究表明, NMLs占乳腺病变的9.2%[7], 其中约27% ~ 68.4%的病例为恶性[8-9], 而常规US对乳腺NMLs的准确度和特异度分别为61.2%和56.1%[10], 明显低于常规US应用于乳腺肿块型病变时的诊断准确率[11]。造成诊断准确率低的主要原因包括病灶超声征象不典型、不适用于乳腺超声BI-RADS分类评估等。目前关于US联合ARFI或CEUS用于NMLs鉴别诊断中的报道较少, 且均为小样本量的研究。本研究扩大了样本量, 进一步研究多模态超声检查在乳腺NMLs良恶性鉴别诊断中的应用价值。

　　本研究单因素分析结果显示, 49岁以上、结构扭曲、微钙化、腋窝异常淋巴结、高SWV、高增强均为NMLs为恶性病变的危险因素, 与以往研究结果相似[12-13]。本研究根据病灶灰阶超声特征, 将病灶分为Ⅰ ~ Ⅴ类, 其中表现为低回声区伴微钙化的Ⅰb类和Ⅱb类病灶的恶性比例为82.3%和77.8%, 远高于不伴微钙化的病灶, 伴有微钙化的NMLs病灶恶性风险大大增加。对于不伴有钙化的NMLs, 不同类型的病灶恶性风险为11.8% ~ 44.4%, 仅凭常规超声诊断困难。本研究通过联合CEUS及ARFI, 可以检出86.4%的恶性病例, 所以, 对于伴有钙化的NMLs, 均建议行病理学检查以明确诊断, 而对于不伴有钙化的NMLs, 可以结合CEUS及ARFI, 以提高诊断效果。

　　HSU等[6]依据超声图像表现, 将乳腺NMLs的超声图像特征分为4种类型。笔者在临床工作中发现, 少部分NMLs超声图像没有减弱回声区, 仅伴有可疑微钙化。此类病例多数为乳腺钼靶或增强磁共振检查发现病灶后, 为指导穿刺活检而行超声多模态检查的病例。笔者将此类病例分为第Ⅴ型。本组病例中, Ⅴ型病例共16例, 其中7例为恶性, 恶性病例中5例表现为高增强, 3例SWV≥4.28 m/s, 通过超声多模态检查, 有助于乳腺NMLs中Ⅴ型病例的检出, 利于指导穿刺部位, 精准取材, 提高诊断准确率。

　　肿瘤新生血管的形成是肿瘤发生及发展的基础, 乳

表 4　超声多模态检查对不典型NMLs的诊断效能

Table 4　Diagnostic efficiency of ultrasonic multimodal examination of atypical NMLs

Type	ARFI/CEUS*	Pathological examination/case		Sensitivity	Specificity	Accuracy rating
		Malignant	Benign			
Ⅰa	Malignant	20	25	80.0%	66.2%	69.7%
	Benign	5	49			
Ⅱa	Malignant	23	18	95.8%	75.0%	80.2%
	Benign	1	54			
Ⅲ	Malignant	7	5	87.5%	50.0%	66.7%
	Benign	1	5			
Ⅳ	Malignant	2	5	100%	66.7%	70.6%
	Benign	0	10			
Ⅴ	Malignant	5	4	71.4%	60.0%	64.7%
	Benign	2	6			
Total	Malignant	57	57	86.4%	68.5%	73.3%
	Benign	9	124			

* When the lesion scored 4 or 5 in CEUS or SWV≥4.28 m/s in ARFI, it was considered malignant.

腺癌发生发展过程中, 肿瘤新生血管的形成早于形态学的改变, 所以, 通过CEUS检查, 评估乳腺NMLs, 有助于乳腺良恶性病变的早期鉴别诊断[14-15]。与良性病变相比, 恶性NMLs在CEUS检查时, 往往表现为开始增强的时间早、增强程度更高、增强范围扩张及伴有放射状滋养血管等[16-18]。这与肿块型乳腺癌表现类似[19]。然而, 需要注意的是仅表现为高增强的造影评分为3分的病例中, 仍有37.7%(26/69)的病例为恶性, 其中20.3%(14/69)为导管内癌, 恶性比例远高于CEUS评分为3分的肿块型病例, 这可能与NMLs病例中早期导管原位癌病例比例远高于肿块型病例有关[20]。所以, 对于CEUS表现为高增强的乳腺非肿块型病例, 均需联合超声多模态征象综合评估, 以防早期恶性病灶的误诊。

本研究发现, US联合ARFI及CEUS的诊断价值最高。对于US检查病灶明确的病例, 可以联合ARFI检查, 提高诊断效能; 对于US检查不明显的病例, 建议联合ARFI和CEUS检查, 既有利于提高诊断效果, 又有利于指导穿刺活检, 精准取材, 为临床医师进一步的诊疗决策提供更精准的依据。

<center>*　　　*　　　*</center>

作者贡献声明　王慧妍负责调查研究和初稿写作, 陆龙颖负责数据审编、调查研究和提供资源, 张和庆、万雪、何玉霜、骆洪浩和彭玉兰负责调查研究和提供资源, 马琳负责正式分析、调查研究和提供资源, 赵海娜负责论文构思、数据审编、经费获取、研究方法、研究项目管理、监督指导和审读与编辑写作。所有作者已经同意将文章提交给本刊, 且对将要发表的版本进行最终定稿, 并同意对工作的所有方面负责。

Author Contribution　WANG Huiyan is responsible for investigation and writing--original draft. LU Longying is responsible for data curation, investigation, and resources. ZHANG Heqing, WAN Xue, HE Yushuang, LUO Honghao, and PENG Yulan is responsible for investigation and resources. MA Lin is responsible for formal analysis, investigation, and resources. ZHAO Haina is responsible for conceptualization, data curation, funding acquisition, methodology, project administration, supervision, and writing--review and editing. All authors consented to the submission of the article to the Journal. All authors approved the final version to be published and agreed to take responsibility for all aspects of the work.

利益冲突　所有作者均声明不存在利益冲突

Declaration of Conflicting Interests　All authors declare no competing interests.

<center>**参　考　文　献**</center>

［1］ 王知力, 唐杰, 李俊来, 等. 乳腺非肿块型病变的超声诊断. 中国医学影像学杂志, 2013, 21(1): 13–15. doi: 10.3969/j.issn.1005-5185.2013.01.004.
WANG Z L, TANG J, LI J L, et al. Ultrasound diagnosis of non-mass-like breast lesions. Chin J Med Imaging, 2013, 21(1): 13–15. doi: 10.3969/j.issn.1005-5185.2013.01.004.

［2］ CHA H, CHANG Y W, LEE E J, et al. Ultrasonographic features of pure ductal carcinoma in situ of the breast: correlations with pathologic features and biological markers. Ultrasonography, 2018, 37(4): 307. doi: 10.14366/usg.17039.

［3］ ASSING M A, PATEL B K, KARAMSADKAR N, et al. A comparison of the diagnostic accuracy of magnetic resonance imaging to axillary ultrasound in the detection of axillary nodal metastases in newly diagnosed breast cancer. Breast J, 2017, 23(6): 647–655. doi: 10.1111/tbj.12812.

［4］ LIU X, WANG M H, WANG Q, et al. Diagnostic value of contrast-enhanced ultrasound for sentinel lymph node metastasis in breast cancer: an updated meta-analysis. Breast Cancer Res Treat, 2023, 202(2): 221–231. doi: 10.1007/s10549-023-07063-2.

［5］ 肖晓云, 智慧, 杨海云, 等. 超声造影5分法诊断乳腺肿物的价值初探. 中华超声影像学杂志, 2012, 21(4): 328–331. doi: 10.3760/cma.j.issn.1004-4477.2012.04.018.
XIAO X Y, ZHI H, YANG H Y, et al. Initial study of contrast-enhanced ultrasound 5-point scoring system in the diagnosis of breast tumor. Chin J Ultrasonogr, 2012, 21(4): 328–331. doi: 10.3760/cma.j.issn.1004-4477.2012.04.018.

［6］ HSU H H, YU J C, LEE H S, et al. Complex cystic lesions of the breast on ultrasonography: feature analysis and BI-RADS assessment. Eur J Radiol, 2011, 79(1): 73–79. doi: 10.1016/j.ejrad.2009.12.037.

［7］ 池月芮, 刘丽, 刘喜艳, 等. 常规超声分型和超声造影在乳腺非肿块型病变中的应用价值. 肿瘤防治研究, 2022, 49(10): 1048-1053. doi: 10.3971/j.issn.1000-8578.2022.22.0128.
CHI Y R, LlU L, LIU X Y, et al. Application value of conventional ultrasound classification and contrast-enhanced ultrasound in non-mass breast-like lesions. Cancer Res Prev Treat, 2022, 49(10): 1048–1053. doi: 10.3971/j.issn.1000-8578.2022.22.0128.

［8］ PARK K W, PARK S, SHON I, et al. Non-mass lesions detected by breast US: stratification of cancer risk for clinical management. Eur Radiol, 2021, 31(3):1693-1706. doi: 10.1007/s00330-020-07168-y.

［9］ UEMATSU T. Non-mass-like lesions on breast ultrasonography: a systematic review. Breast Cancer, 2012, 19(4): 295–301. doi: 10.1007/s12282-012-0364-z.

［10］ 韩龄锋. 多模态超声联合评分法对乳腺非肿块型病变的诊断价值. 重庆: 西南医科大学, 2018.
HAN L F. Diagnostic value of multimodal ultrasound and its combined scoring method for non-lump type lesions of the breast. Chongqing: Southwest Medical University, 2018.

［11］ LI D D, XU H X, GUO L H, et al. Combination of two-dimensional shear wave elastography with ultrasound breast imaging reporting and data system in the diagnosis of breast lesions: a new method to increase the diagnostic performance. Eur Radiol, 2016, 26(9): 3290–300. doi: 10.1007/s00330-015-4163-8.

［12］ 吴小茜, 江燕辉, 刘美伶, 等. 恶性乳腺非肿块型病变超声特征分析及列线图预测模型构建. 实用医学杂志, 2023, 39(1): 119–123. doi: 10.3969/j.issn.1006-5725.2023.01.021.

WU X X, JIANG Y H, LIU M L, *et al*. Analysis of ultrasound characteristics of malignant breast non-mass-like lesins and development of a nomogram. J Pract Med, 2023, 39(1): 119–123. doi: 10.3969/j.issn. 1006-5725.2023.01.021.

［13］ LI M, LI Q, YIN Q, *et al*. Evaluation of color Doppler ultrasound combined with plasma miR-21 and miR-27a in the diagnosis of breast cancer. Clin Transl Oncol, 2021, 23(4): 709–717. doi: 10.1007/s12094-020-02501-9.

［14］ 周雅筠, 谢瑾, 张蓓, 等. 常规超声、超声造影、钼靶X线、磁共振成像及联合检测对早期乳腺癌患者的诊断价值. 贵州医科大学学报, 2023, 48(2): 172–176. doi: 10.19367/j.cnki.2096-8388.2023.02.008.

ZHOU Y Y, XIE J, ZHANG B, *et al*. Diagnostic values of conventional ultrasound, contrast-enhanced ultrasound, mammography, magnetic resonance imaging and their combinations in diagnosing patients with early breast cancer. J Guizhou Med Univ, 2023, 48(2): 172–176. doi: 10. 19367/j.cnki.2096-8388.2023.02.008.

［15］ TOZAKI M, ISOBE S, YAMAGUCHI M, *et al*. Ultrasonographic elastography of the breast using acoustic radiation force impulse technology: preliminary study. Jpn J Radiol, 2011, 29(6): 452–456. doi: 10. 1007/s11604-011-0561-2.

［16］ 王洲, 刘芳欣, 殷延华, 等. 声触诊组织成像定量技术联合超声造影诊断乳腺原发性淋巴瘤1例. 中国医学影像技术, 2021, 37(1): 157. doi: 10. 13929/j.issn.1003-3289.2021.01.040.

WANG Z, LIU F X, YIN Y H, *et al*. Virtual touch tissue imaging quantification combined with contrast-enhanced ultrasound in diagnosis of breast primary lymphoma: case report. Chin J Med Imag Tech, 2021, 37(1): 157. doi: 10.13929/j.issn.1003-3289.2021.01.040.

［17］ 马丹丹, 王涛, 刘国岩, 等. 乳腺造影评分法校正分类对乳腺肿块的鉴别价值. 长春中医药大学学报, 2023, 39(11): 1262–1265. doi: 10.13463/j. cnki.cczyy.2023.11.019.

MA D D, WANG T, LIU G Y, *et al*. Value of correcting the classification of mammography scoring method in distinguishing benign and malignant breast masses. J Changchun Univ Tradit Chin Med, 2023, 39(11): 1262–1265. doi: 10.13463/j.cnki.cczyy.2023.11.019.

［18］ 闫玉琪, 欧笛, 倪晨, 等. 超声造影及相关新技术在乳腺癌诊疗中的研究进展. 肿瘤影像学, 2023, 32 (6): 561–566. doi: 10.19732/j.cnki.2096-6210.2023.06.013.

YAN Y Q, OU D, NI C, *et al*. Research progress of contrast-enhanced ultrasound and related new technologies in the diagnosis treatment of breast cancer. Oncoradiology, 2023, 32 (6): 561–566. doi: 10.19732/j.cnki. 2096-6210.2023.06.013.

［19］ 张庆坤, 冷晓玲, 张芬, 等. 超声造影对早发性乳腺癌的诊断价值. 中国超声医学杂志, 2015, 31(4): 305–307.

ZHANG Q K, LENG X L, ZHANG F, *et al*. Diagnostic value of contrast-enhanced ultrasonography in early-onset breast cancer. Chin J Ultrasound Med, 2015, 31(4): 305–307.

［20］ OLENA W, WEI Y. Imaging of breast cancers with predilection for nonmass pattern of growth: invasive lobular carcinoma and DCIS--does imaging capture it all? AJR, 2020, 215(6): 1504–1511. doi: 10.2214/AJR.19. 22027.